

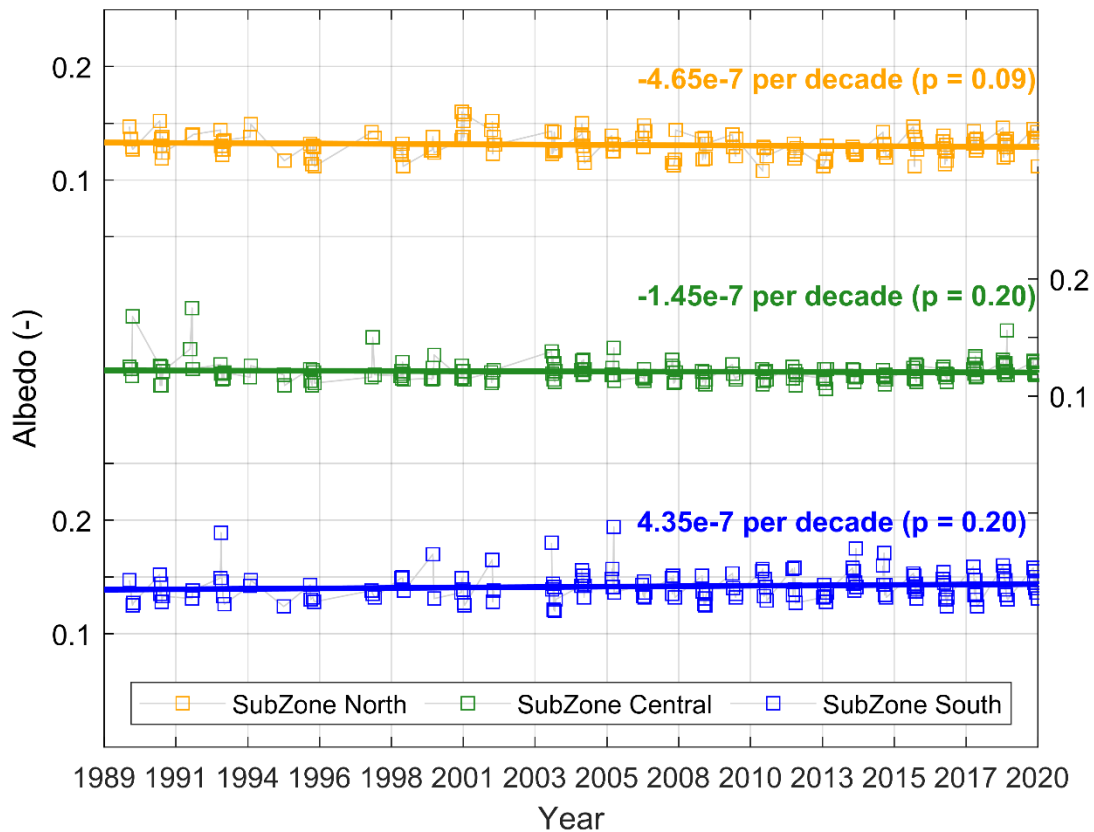
1 **Supplementary Information for:**
 2 **Glacier albedo reduction and drought effects in the extratropical**
 3 **Andes, 1986-2020**

4
 5
 6 Thomas E. Shaw^{1,2}, Genesis Ulloa³, David Farías-Barahona⁴, Rodrigo Fernandez³, Jose M.
 7 Lattus^{3,5}, James McPhee^{3,6}

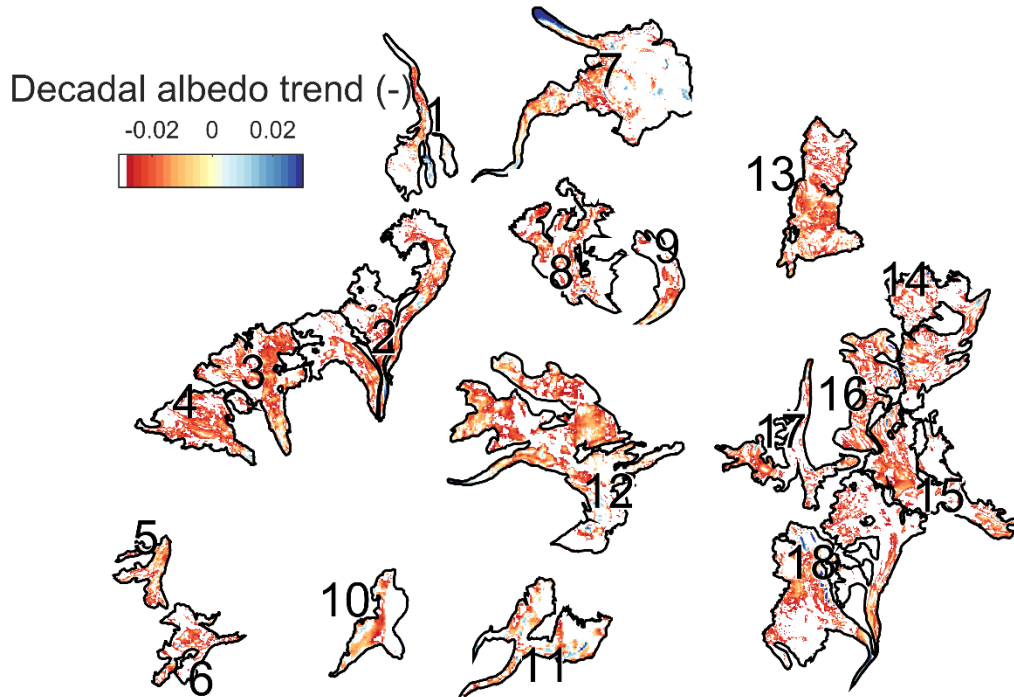
8
 9 %%%%%%%%%%%%%%%%%%%%%%%%%%%%%%%%%%%%%%%%%%%%%%%%%%%%%%%%%%%%%%%%%%%%%%%%%%

10
 11 Contents:

- 12
 13 1) Figure S1 – Consistency of albedo derived from equation 1 of text for all, Landsat scenes
 14 between 1989-2020 at AWS pixels in each sub-zone (see main text)
 15 2) Figure S2 – pixel-by-pixel trends of glacier albedo per decade.
 16 3) Figure S3 – As Figure 4 of main text, but for individual glaciers. Mean, all-year albedo per
 17 elevation band and the relative changes in mean albedo for the 2010-2020 period and 2020
 18 only.
 19 4) Figure S4 – As Figure S3, but showing the hypsometry of each glacier.
 20 5) Figure S5 – An experiment of estimated melt rates from an ETI model approach using different
 21 albedo maps of the 2020 summer melt season on Juncal Sur Glacier.
 22 6) Text to explain the set-up of the simplified ETI model.

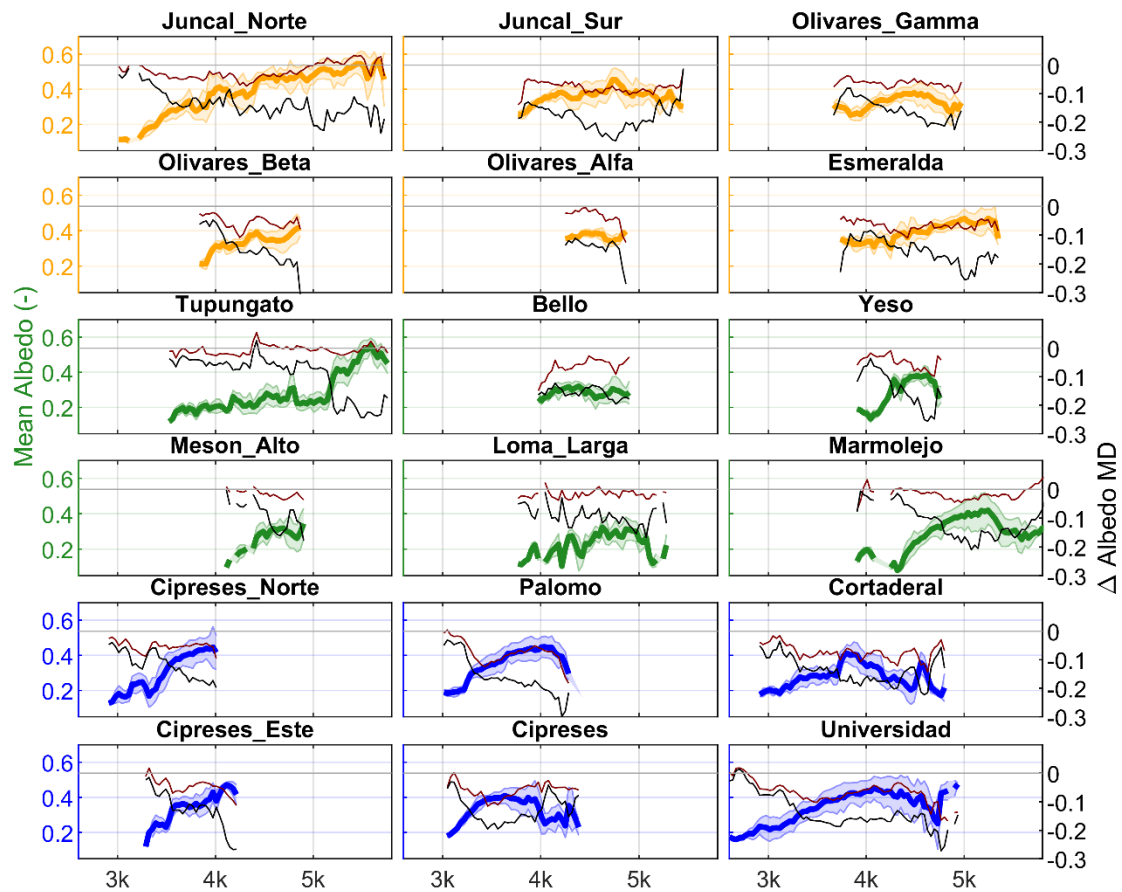


23
 24 *Figure S1: The sensor consistency in measuring end-of-winter broadband shortwave albedo at off-glacier*
 25 *locations in each sub-zone, Olivares Gamma (orange), Laguna Negra (green) and Cortaderal (blue). Trends are*
 26 *negligible and significant to the 0.8 level.*
 27



28
29
30
31
32
33
34
35

Figure S2: Decadal trends in pixel-by-pixel albedo for all years excluding those with early snowfall occurrence (see Figure 3 of main text). Areas of white indicate where trends through linear regression were not significant to the 0.8 level of higher. This was largely the result of data loss due to shadowing or saturation for high elevation areas of glaciers such as Juncal Norte (1), Tupungatito (7), Marmolejo (12) and Universidad (18). Artefacts on Tupungatito (7) resulted in missing data for some OLI scenes and thus a strong positive trend in albedo change.



36
 37
 38
 39
 40
 41

Figure S3: The all-year mean albedo per elevation band (50m) for all glaciers (coloured lines) and the standard deviation of all years for each glacier. The right hand axes show the elevation-mean differences of the mega-drought ('MD' 2010-2020 in brown) and 2020 (black) relative to 1989-2009. Orange bars denote the 0.025 uncertainty threshold for change detection.

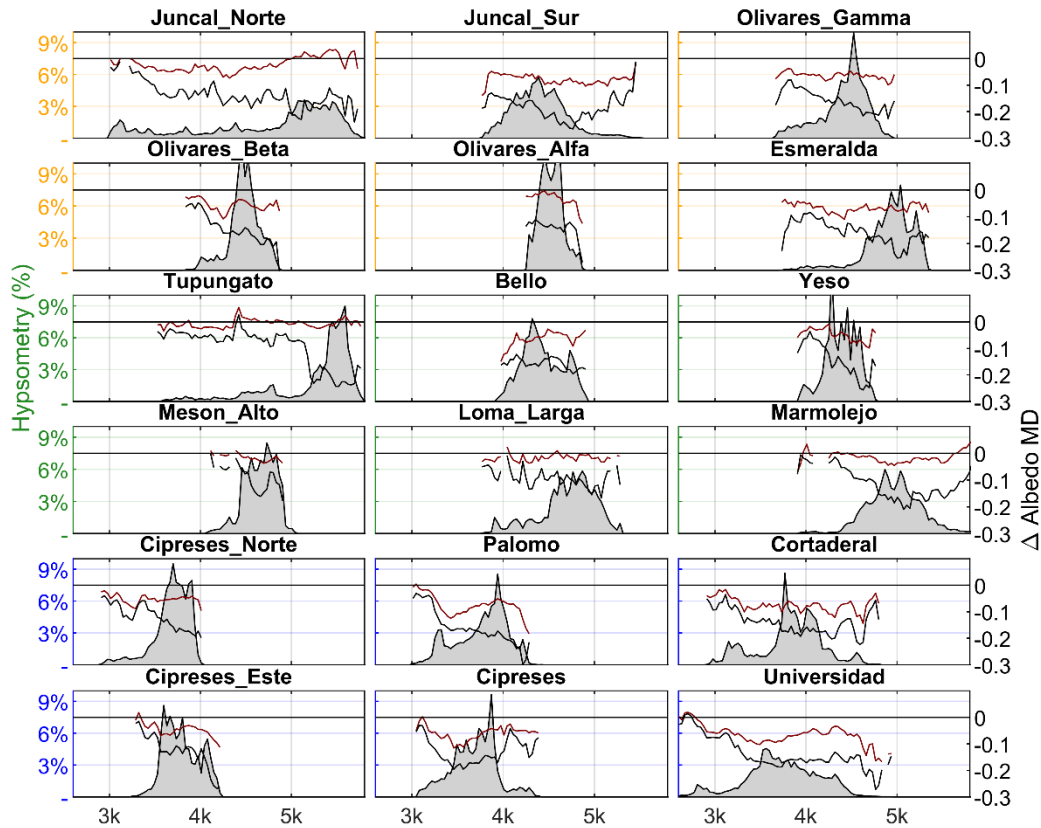


Figure S4: As Figure S3, but showing the hypsometry (grey shaded area) of each glacier (% area of total per 100 m DEM band – left axis) vs the changes during the MD and 2020 periods (right axis – identical to Figure S3).

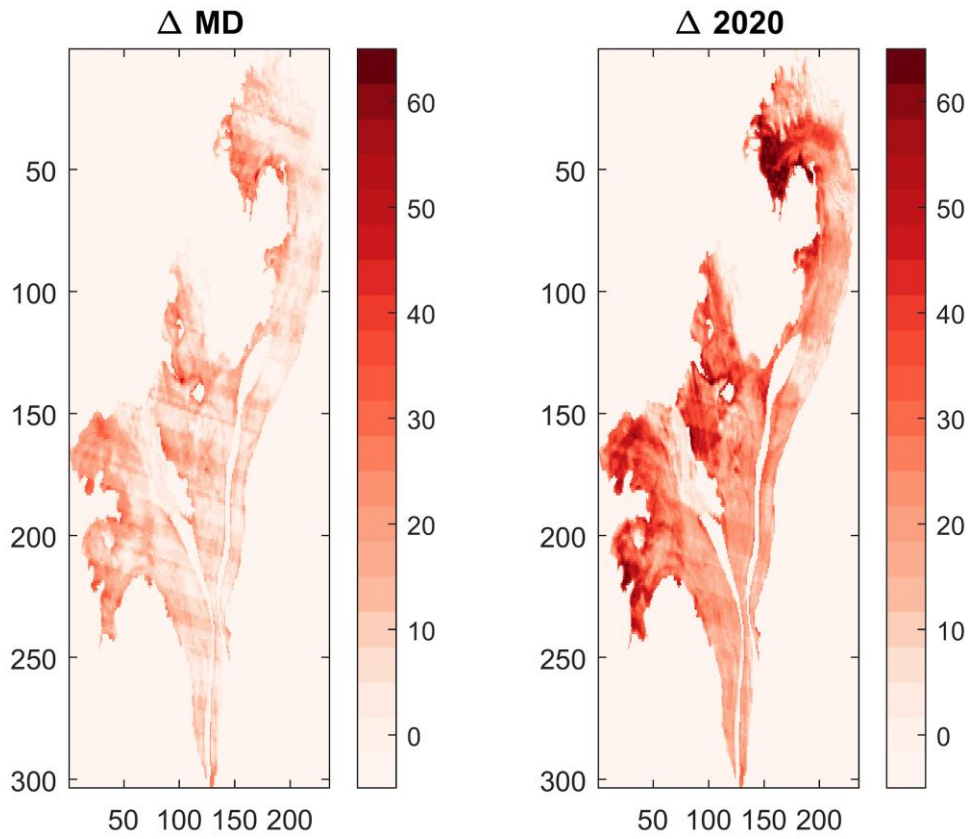
42
43
44
45
46
47
48
49
50
51
52
53
54
55
56
57
58
59
60
61
62
63
64
65
66
67
68
69
70
71

Application of a simple melt model

We apply the Enhance Temperature Index (ETI) model of Pellicciotti and others (2005) to model the surface melt of Juncal Sur Glacier during the end-of-summer 2020 (1st March - 30th April) considering different albedo scenarios derived from the LandSat data (see main text). The ETI model follows the form:

$$Melt = TF \cdot Ta + SRF \cdot (1 - Albedo) \cdot Swin$$

where TF ($\text{mm h}^{-1} \text{ } ^\circ\text{C}^{-1}$) and SRF ($\text{m}^2 \text{ mm W}^{-1} \text{ h}^{-1}$) are the respective temperature and shortwave radiation factors for computing melt, Ta is the air temperature and $Swin$ is the incoming shortwave radiation. We refer the reader to Pellicciotti and others (2005) for specific model details. We utilised the hourly meteorological information at the off-glacier Olivares Gamma AWS (Figure S1) for Ta and $Swin$ and Albedo information was derived from the LandSat data. We assumed $Swin$ to be spatially constant and distributed Ta over the glacier elevations (ASTER GDEM) using a lapse rate of $-0.0065^\circ\text{C m}^{-1}$ and a temperature offset of 1°C to account for the glacier boundary layer. We compare the summed melt rates of the two-month period assuming; i) the static mean albedo of the 1986-2009 period; ii) the static mean albedo of the MD period (2010-2020) or; iii) the 2020 albedo values. Figure S4 shows the relative differences in pixel-wise melt of the MD and 2020 years compared to the 1986-2009 mean albedo. It is noted that some pixels highlight a potential difference in melt rates $>60\%$ for the 2020 albedo grid. On average the differences are 9.8% and $\sim 20\%$ greater when considering the albedo grids of the MD and 2020, respectively compared to the 1986-2009 average. This is a simplified exercise that assumes the same meteorological conditions regardless of glacier albedo and is subject to many simplifications. Nevertheless, the model is utilised only as a general example of the importance of glacier albedo reduction for the mass and energy balance of these glaciers.



72
 73
 74
 75
 76
 77
 78

Figure S5: The change (%) in calculated melt of Juncal Sur Glacier during March-April 2020 considering the MD average albedo (left) and the 2020 albedo relative to the mean 1986-2009 albedo.